

Shelter site location under multi-hazard scenarios

Eren Ozbay^{a,1}, Özlem Çavuş^{b,*}, Bahar Y. Kara^b

^a College of Business Administration, University of Illinois at Chicago, Chicago, IL 60607, USA

^b Department of Industrial Engineering, Bilkent University, Ankara 06800, Turkey

ARTICLE INFO

Article history:

Received 8 September 2017

Revised 3 January 2019

Accepted 17 February 2019

Available online 21 February 2019

Keywords:

Shelter site location

Secondary disasters

Multi-stage stochastic programming

Conditional value-at-risk

ABSTRACT

Natural disasters may happen successively in close proximity of each other. This study locates shelter sites and allocates the affected population to the established set of shelters in cases of secondary disaster(s) following the main earthquake, via a three-stage stochastic mixed-integer programming model. In each stage, before the uncertainty in that stage, that is the number of victims seeking a shelter, is resolved, shelters are established, and after the uncertainty is resolved, affected population is allocated to the established set of shelters. The assumption on nearest allocation of victims to the shelter sites implies that the allocation decisions are finalized immediately after the location decisions, hence both location and allocation decisions can be considered simultaneously. And, when victims are allocated to the nearest established shelter sites, the site capacities may be exceeded. To manage the risk inherent to the demand uncertainty and capacities, conditional value-at-risk is utilized in modeling the risk involved in allocating victims to the established shelter sites. Computational results on Istanbul dataset are presented to emphasize the necessity of considering secondary disaster(s), along with a heuristic solution methodology to improve the solution qualities and times.

© 2019 Elsevier Ltd. All rights reserved.

1. Introduction

From the beginning of 20th century, more than the current population of the world has been affected by various natural disasters (EM-DAT, 2008). In the recent years, the literature on disaster operations management (DOM) has grown bigger. The reader is referred to Altay and Green (2006), Caunhye et al. (2012), Galindo and Batta (2013), Hoyos et al. (2015), and the references therein for the details.

The DOM literature is classified into four main phases: (i) mitigation, (ii) preparedness, (iii) response, and (iv) recovery (McLoughlin, 1985). Phases (i) and (ii) refer to pre-disaster, while phases (iii) and (iv) refer to post-disaster operations. The mitigation phase involves the actions taken in order to prevent and mitigate the consequences of a possible disaster. The preparedness phase includes plans for specific cases and provides effective responses to disasters. After a disaster occurs, the response phase deals with providing the affected population with relief goods and primary needs, such as water, food, medical care, shelter, etc. Lastly, the recovery phase aims to recover all the damaged

(infra)structure in order to ensure the normal functioning of the affected population.

In this study, the emphasis is on the people who cannot stay their homes after an earthquake has occurred and seek accommodation in temporary shelters. To accommodate the disaster victims, one has to devote certain safe areas to establish temporary shelters. Usually, this decision of choosing candidate shelter locations is made before a disaster occurs, and the decision of establishing some combination of them is made after the disaster but before the observation of the actual demand. The demand uncertainty and the importance of choosing the best locations for shelters make this problem one of the fundamental facility location problems in the preparedness phase of DOM. This problem is known in the literature as the shelter site location problem (Kılıcı et al., 2015).

It is important to consider the features of the network while creating a methodology to locate shelter sites to host disaster victims, e.g. the distance between the potentially affected population and the shelter sites or the capacity of shelter sites. 1999 Marmara Earthquake provides an example for the case where the population hosted in the shelters exceeds the shelter capacities as much as 40% (Kılıcı et al., 2015). The problems that were observed in 1999 Marmara Earthquake motivated several studies, such as JICA report (Cavdur et al., 2016; Görmez et al., 2011; JICA, 2002; Kılıcı et al., 2015).

Although it was not as apparent in 1999 Marmara Earthquake, in some cases of disasters, the size of the displaced population

* Corresponding author.

E-mail addresses: eozybay3@uic.edu (E. Ozbay), ozlem.cavus@bilkent.edu.tr (Ö. Çavuş), bkara@bilkent.edu.tr (B.Y. Kara).

¹ Eren Ozbay was an MSc student at the Department of Industrial Engineering, Bilkent University, Ankara, Turkey when this research was conducted.

may grow larger because of the secondary disaster(s) following the main shock. For 1999 Marmara Earthquake, secondary disasters were a disastrous fire at the Tüpraş petroleum refinery, tsunami in the Marmara sea, and the strong earthquake in Düzce (Al Jazeera Turk, 2013). Similarly, the destructive aftershock in Van-Erdremi, which took place 17 days after the Van-Erciş Earthquake, is another example of secondary disasters (Al Jazeera Turk, 2013). When the nature of consecutive disasters are analyzed, it can be observed that the main and secondary disasters might be of same types (e.g. aftershocks following an earthquake as in Illapel Earthquake, 2015) or of different types (e.g. tsunamis coupled with nuclear meltdown following an earthquake as in Tōhoku Earthquake, 2011). In the literature, this phenomenon of having consecutive disasters is called multi-hazard, which is defined as the combination of various hazards in a defined area (Kappes et al. (2010, 2012)).

In this study, we consider the multi-hazard phenomenon in the context of the shelter site location problem. We focus only on the earthquakes, namely the main shocks and the aftershocks. Therefore, for the rest of the study, we will use aftershock and secondary disaster interchangeably.

For the purpose of our study, the magnitudes of the aftershocks and the time between two shocks are two important questions to be answered. In the related literature, there is a handful of well-established empirical laws relating the magnitudes of aftershocks and rate to time after the main shock, most eminent ones being Omori's (1894), Bath's (1965), and Gutenberg and Richter (1954) laws. Omori's law states that the number of aftershocks decreases nearly hyperbolically with time. Bath's law concludes that the largest aftershock is usually about one magnitude unit smaller than the main shock. Gutenberg-Richter law mainly points out that more small and fewer large magnitude aftershocks occur. Therefore, in this study, we only consider destructive aftershocks and assume that at most one destructive aftershock can occur after the main shock and it affects a smaller percentage of people with respect to the main shock. One may question the time between the main earthquake and the largest aftershock. According to Utsu (1970), for a main earthquake with a magnitude of 7, the time difference is generally in the range 0.01–100 days and the range gets larger with the magnitude of main shock. To give examples, for 1999 Marmara Earthquake, the largest aftershock is 27 days later than the main shock (Örgülü and Aktar, 2001), and this time is 17 and 32 days for 2015 Nepal (Wikipedia, 2018) and 2016 Ecuador (Wu et al., 2017) earthquakes, respectively.

The decision of establishing some combination of the candidate shelter sites becomes more complicated as the demand uncertainty created by the main shock couples with the demand uncertainty created by the possible aftershock. We investigate the effect of this kind of stochasticity on the shelter site location problem. As it is in the real setting, we assume that the decision maker (DM) locates the shelter sites in the first stage, that is after the main earthquake and before the realization of the actual demand. After the realization of the demand, in the second stage, the allocation of disaster victims to the shelter sites are made. Then, again in the second stage, we consider that in case of an aftershock hitting the area, the DM is required to decide whether or not to establish new shelter sites to meet the new (aftershock) demand. Finally, in the third stage, after whole uncertainty is resolved, the allocation of disaster victims affected by the aftershock to the shelter sites are made and utilization of shelter sites are observed. We assume that in the preparedness phase, the candidate shelter site locations have already been determined and the shelters, which usually are tents, are ready to be established promptly after the earthquake. Shelters can be established within a few days after the earthquake; for example, it was two days in the 2011 Van Earthquake (Milliyet, 2011). Based on the discussion on time difference between main shock and the largest aftershock, we assume that the largest aftershock

occurs after the shelter sites due to main earthquake are established.

In order to model the behavior of the disaster victims in a more realistic manner, we assume that the disaster victims in the same neighborhood will always travel to the same nearest shelter site. In this setting, the allocation decision of victims to the shelter sites can be made as soon as the shelter sites are located. Hence, the allocation decisions are made implicitly and they follow the location decisions. So, in our setting, we can discuss that the location and allocation decisions regarding the main earthquake are made in the first stage and the location and allocation decisions regarding the aftershock are made in the second stage, after the main earthquake demand is realized. In the third stage, after the whole uncertainty is resolved, the utilizations of shelter sites are observed.

Note that, from a psychological point of view, it is possible that a certain portion of the disaster victims –who are to reside in the shelters after the aftershock– may choose to travel to a farther shelter site, that has been established in the first stage, to be with their neighbors. Since this approach would require parametric analysis on the portion of population that embraces such a choice, we preserve the nearest assignment idea throughout this study.

When the disaster victims are *always* assigned to the nearest shelter site without demand division, the shelter site capacities may be exceeded. So, we define the risk in this setting as the capacity of a shelter site being exceeded. We utilize the conditional value-at-risk (CVaR, as introduced by Rockafellar and Uryasev (2000)) as the risk measure to quantitatively represent the risk and experiment with varying quantile levels to observe the behavior of the model. The analyses presented later in the study suggest that it is in fact important to consider the secondary disasters while locating the shelter sites.

The remainder of this paper is organized as follows: in Section 2, the relevant literature related to this study is reviewed. In Section 3, the proposed three-stage stochastic mixed-integer programming (MIP) model is presented. Section 4 is devoted to the details of the dataset creation for a district of Istanbul. The results of the problem instances are presented and discussed in Section 5. A heuristic solution methodology to improve the solution qualities and times is proposed in Section 6. In Section 7, we present the value of using the three-stage model. The paper is concluded with an overview of the study and future research directions.

2. Literature review

Facility location decisions are often costly and almost always irreversible, and since the parameters, such as demand, that they abide may fluctuate, stochastic modeling is very relevant (Snyder, 2006). While reviews by Owen and Daskin (1998) and Current et al. (2002) examine both deterministic and stochastic facility location models, Snyder (2006) and Caunhye et al. (2012) discuss only stochastic nature of facility location problems and all agree that the complexity of location problems are captured best by stochastic modeling.

With an enormous literature on facility location, the application of those models to humanitarian logistics is abundant (see, e.g. Altay and Green, 2006; Simpson and Hancock, 2009; Galindo and Batta, 2013), especially with an emphasis on humanitarian logistics, as can be seen in Özdamar et al. (2004), Kovács and Spens (2007), and Leiras et al. (2014).

The review papers by Ortuño et al. (2013), Liberatore et al. (2013), and Grass and Fischer (2016) indicate the essence of the effects that stochasticity creates in humanitarian logistics. The review by Liberatore et al. (2013) defines the risks and uncertainties associated with disasters in depth, and furthermore, discusses the sources of uncertainties in disasters and how to model them.

Table 1
Deterministic location studies in humanitarian logistics.

Article	Single/Multi Objective	Objective(s)	Decision(s)	Solution Methodology
Kilci et al. (2015)	S	Shelter weight	Location, Allocation	MIP solver
Bayram et al. (2015)	S	Evacuation time	Location, Allocation, Evacuation	2 nd order cone programming
Kongsomsaksakul et al. (2005)	S	Evacuation time	Location, Allocation, Evacuation	Genetic algorithm
Chanta and Sangsawang (2012)	M	Weighted distance, maximum cover	Location, Allocation	MIP solver
Alçada-Almeida et al. (2009)	M	Distance, risk, evacuation time	Location, Allocation, Evacuation	MIP solver
Coutinho-Rodrigues et al. (2012)	M	Distance, risk, evacuation time	Location, Allocation, Evacuation	MIP solver

Table 2
Stochastic shelter site location studies in humanitarian logistics.

Article	# of Stages	Objective(s)	Decision(s)	Uncertainty	Solution Method
Bayram and Yaman (2018)	2	Expected evacuation time	F: Location S: Evacuation	Demand, disruption in transport network and shelter sites	MIP solver
Li et al. (2011)	2	LC, TC _e , IC _e , PC _e , AC _e	F: Location, Capacity S: Allocation	Demand, commodity transportation and evacuee allocation cost	L-Shaped method
Li et al. (2012)	2	S: Expected unmet demand, Expected travel time	F: Location S: Evacuation	Demand, shelter, accessibility, time	Heuristic
Our Model	3	Number of expected-weighted shelter sites	F: Location, Allocation S: Location, Allocation T: Utilization	Demand	Heuristic

Grass and Fischer (2016), on the other hand, survey only two-stage stochastic models in disaster management in depth and provide details on the general framework. These surveys provide a basis for the significance of the proposed problem and help in finding crucial and essential research directions to pursue.

The above brief literature shows that the location problem is an emerging problem for DOM (see Rawls and Turnquist, 2010; Rawls and Turnquist, 2011). These problems may be classified as: (i) emergency medical location problem; (ii) relief material (warehouse) location problem; (iii) shelter site location problem (Kilci et al., 2015). Existing literature covers categories (i) and (ii) extensively, leaving category (iii) fairly unexplored. In this work, we focus on category (iii). So, we survey the related literature by dividing it into two main parts; deterministic and stochastic studies in humanitarian logistics, focused primarily on shelter site location problems.

The relevant deterministic studies are summarized in Table 1. The first column introduces the article; the second column states if the study is single-objective or multi-objective (denoted as S/M); the third and fourth columns denote the objective(s) and decision(s) of the study, respectively; lastly the fifth column denotes if the proposed model is solved directly with a commercial solver or the author(s) devise a methodology.

Kilci et al. (2015) address the problem of locating shelter sites for an earthquake case for Istanbul, Turkey. Using predetermined set of weights for shelter sites (weight of a shelter site is simply an indicator for its overall service level), they maximize the minimum weight of the established shelter sites. Bayram et al. (2015) and Kongsomsaksakul et al. (2005) propose models to minimize the total evacuation time by locating shelters and assigning evacuees to shelters. While Bayram et al. (2015) assign evacuees to the nearest shelter sites, within a given degree of tolerance, Kongsomsaksakul et al. (2005) propose a bi-level program with the upper level deciding on the shelter locations and the lower level deciding on the assignment of evacuees to shelters.

Alçada-Almeida et al. (2009) propose a multi-objective location-evacuation model to locate emergency shelter sites and identify evacuation routes with lower and upper limits on shelter site utilizations and predefined number of shelter sites. Coutinho-Rodrigues et al. (2012) extend Alçada-Almeida et al. (2009) by introducing varying objectives and not limiting the number of shelter sites to be opened. Chanta and Sangsawang (2012) investigate a bi-objective model which determines the locations of shelter sites to serve a region suffering from a flood disaster.

Table 2 summarizes the relevant stochastic studies, using the same classification methodology as above. The first column introduces the article; the second column states if the model is two-stage or three-stage; the third and fourth columns denote the objective(s) and decision(s) of the study, respectively, where *F* stands for the first stage, *S* for the second stage, and *T* for the third stage; the fifth column indicates the uncertain parameters; lastly the sixth column denotes if the proposed model is solved directly with a commercial solver or the author(s) devise a methodology.

In humanitarian logistics studies, various types of costs are considered, so we use following abbreviations in Table 2: TC_e is the expected relief material transportation cost; LC is the facility location cost; IC_e is the expected inventory holding cost; AC_e is the expected cost of transporting disaster victims to shelters; and PC_e is the expected penalty cost of unsatisfied demand.

Bayram and Yaman (2018), Li et al. (2011), and Li et al. (2012) propose shelter location models. Li et al. (2011) look at cases where the relief supplies are transported from an already existing set of depots to located shelters along with shelter capacities, where Bayram and Yaman (2018); Li et al. (2012) consider evacuation of victims from disaster points to shelter sites. Bayram and Yaman (2018), extending Bayram et al. (2015), assign evacuees to the nearest shelter sites, within a given degree of tolerance, while Li et al. (2012) deal with the distance traveled by evacuees in the objective function and allow evacuees to be unassigned.

The above literature reveals that shelter site location, especially a study that considers secondary earthquakes, is a research direction still to be explored. To the best of our knowledge, only Zhang et al. (2012) consider secondary disasters directly. But the method they propose is fairly inefficient as they have to repeat their algorithm for each disaster scenario (see Su et al. (2016) for a discussion). While Zhang et al. (2012) allocate relief supplies to disaster nodes, we locate shelter sites and allocate disaster victims so that they receive acceptable levels of service in terms of sheltering. We also manage the risk of exceeding capacities of shelter sites due to uncertain demands of main earthquake and aftershock.

3. Shelter site location under multi-hazard scenarios

Earthquakes are among the disasters of which we do not know the time or magnitude in advance. We do not know if any aftershock will follow the main earthquake, and if it does, again we do not know the time, exact epicenter or magnitude of it. All of

this uncertainty leads to stochastic modeling where both the main earthquake and the aftershock, namely the multi-hazard, involve uncertainty. When this multi-hazard phenomenon does occur, the population at risk will be the disaster victims who seek shelters. We assume that the number of victims seeking a shelter is random. Some proportion of the population at risk will seek shelter after the main earthquake and some others will seek after the aftershock. To model this, we introduce multi-hazard methodology into shelter site location problem via a multi-stage stochastic MIP model.

In this setting, after an earthquake has hit, disaster victims sharing the same neighborhood (used interchangeably with district) always travel to the nearest shelter site. So, the shelter site demand cannot be divided to state that certain victims are to reside in another shelter site. In a multi-hazard setting, this behavior reflects to both the main earthquake and the aftershock. When every district travels to the nearest shelter site in any disaster stage, the capacity of the established shelter sites may be exceeded. As it is apparent in 1999 Marmara Earthquake, having shelter site utilizations as high as 140% reduces the quality of services received by the disaster victims (Kilci et al., 2015) (here utilization of a shelter site is defined as the total number of victims staying in the shelter site divided by the capacity of that shelter site).

To manage the risk of exceeding the shelter site capacities, we utilize CVaR constraints. CVaR is first introduced by Rockafellar and Uryasev (2000). Presented as an approach to optimize or hedge a portfolio of financial instruments to reduce risk, CVaR is also used in humanitarian logistics literature to mitigate possible risks (e.g. Noyan, 2012). CVaR, in our setting, provides the DM a way of controlling the risk-aversion level, aiding in management of the over-utilization of shelter sites. As Rockafellar and Uryasev (2000, 2002) discuss, value-at-risk (VaR), another measure of risk, may provide poor quality solutions with respect to CVaR as VaR disregards the distribution of the tail, i.e. may regard higher and smaller violations of the shelter site utilizations as the same and therefore may perform worse.

Having described the problem setting, the proposed model locates shelter sites after a main earthquake and a possible aftershock. It is assumed that the DM decides on the location of the shelter sites after an earthquake has happened and before the actual demand is observed. This is same for the first and second stages. After the demand of the main earthquake and the aftershock are realized in second and third stages, respectively, the allocation decisions are finalized. Lastly, in the third stage, the utilizations of shelter sites are observed.

In our mathematical model, we incorporate nearest assignment, or nearest allocation, constraints to reflect the real life choices of the disaster victims. When the disaster victims travel to the nearest established shelter site, the location decisions imply allocation decisions, i.e. allocation decisions can be made automatically once location decisions are finalized. Therefore, in this case, it does not matter to allocate victims before or after the uncertainty is resolved. So, the allocation decisions regarding the main earthquake can be made in the first stage and the allocation decisions regarding the aftershock can be made in the second stage. We provide our mathematical model under this simplifying observation.

We can illustrate the problem setting using Figs. 1a–1e. The red squares represent the shelter sites, the blue circles represent the demand points (districts) and the yellow star represents the epicenter of the main earthquake. As it is described further in Section 4, all of the possible main earthquakes share the same epicenter. All the demand points in Kartal, Istanbul and the epicenter of the main earthquake can be observed in Fig. 1a.

Once the main earthquake occurs in the first stage, the DM establishes the shelter sites, red squares, before observing the actual demand, as in Fig. 1b, in the first stage. Then, in the same (first)

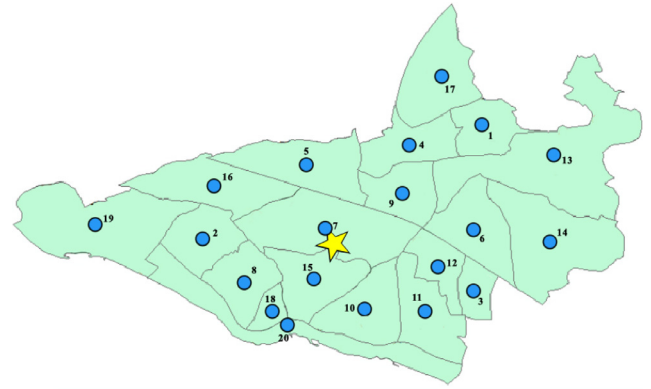


Fig. 1a. Demand points and the epicenter of the main earthquake.

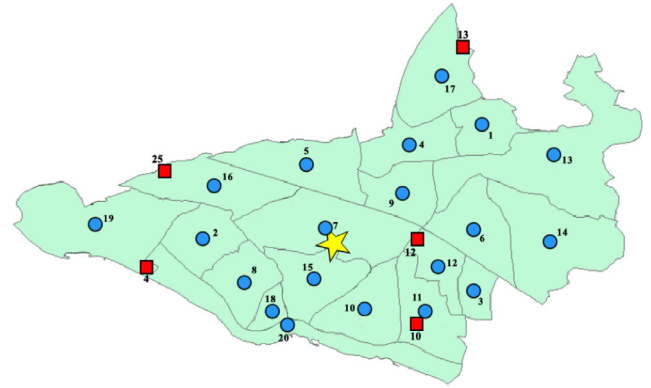


Fig. 1b. Open shelter sites after the main earthquake has occurred.

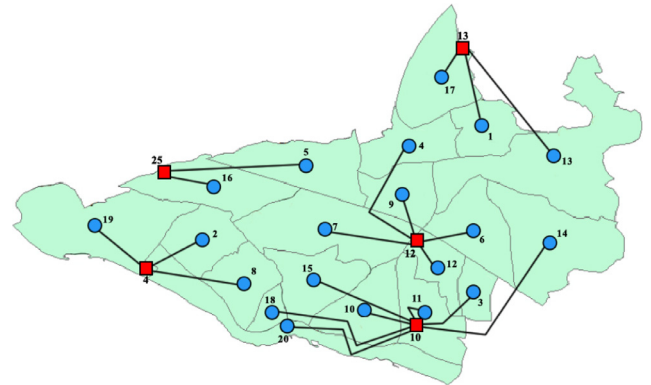


Fig. 1c. Allocation of demand points after the main earthquake has occurred.

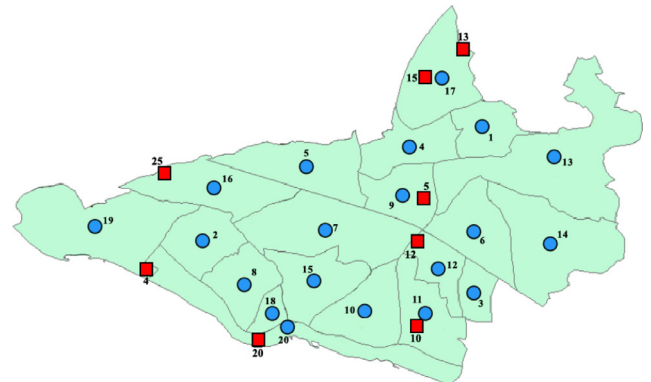


Fig. 1d. Open shelter sites after the aftershock, note that some shelter sites were already open.

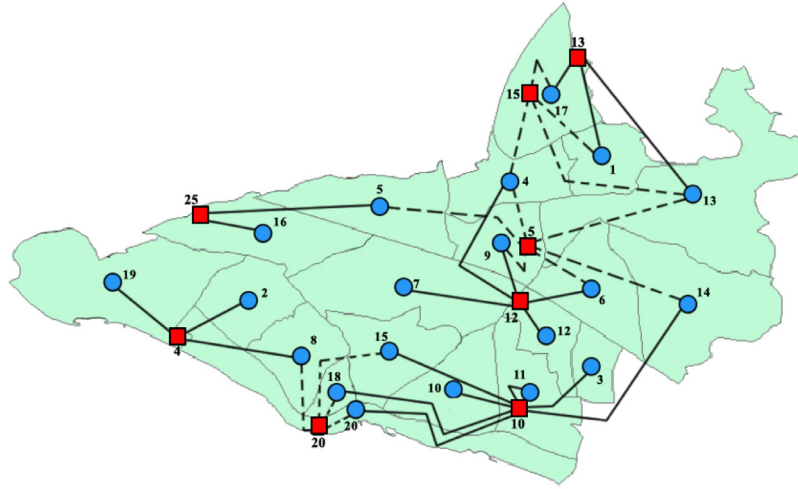


Fig. 1e. Allocation of demand points after the aftershock and the final result of a problem instance.

stage, the allocation of disaster victims to the nearest open shelter sites is as in Fig. 1c – lines represent the allocation of the districts to the open shelter sites. After the disaster victims have traveled to the nearest open shelter site, an aftershock may hit Kartal and may require new shelter sites, additional red squares, to be established, as in Fig. 1d. For this particular instance, three new shelter sites are established. Note that, under some main earthquake demand realizations, some of these three shelter sites may not be established. In the same (second) stage, the allocation of disaster victims to the nearest open shelter site is as in Fig. 1e – dashed lines represent the allocation of the districts to the open shelter sites. As under different disaster scenarios, different shelter sites can be established in the second stage and hence second stage allocation of districts vary among different main earthquake demand realizations. This fact can be observed in Fig. 1e. Districts 4 and 13 have two dashed lines, depending on which shelter site is opened in the second stage.

Throughout this study, we assume that the demand after the main earthquake and the aftershock is uncertain. To the best of our knowledge, in the humanitarian logistics studies, there is not any dataset that considers secondary disasters, although many do consider main disasters (see e.g. Balcik and Beamon, 2008; Gunnec and Salman, 2007; Kılıcı et al., 2015; Noyan et al., 2015; Verma and Gaukler, 2015). Therefore, we create a new dataset based on the network provided by Kılıcı et al. (2015). We assume that an aftershock may follow a main earthquake. We provide a dataset where a scenario corresponds to a main earthquake-aftershock demand realization pair.

After preliminary tests with the proposed mathematical model using the proposed dataset, we seek to improve the quality of solutions as victims are assigned to farther shelter sites and some shelter sites have utilizations as low as 3% in some instances. To remedy this, we consider including two additional set of constraints to the formulation: an upper limit on the distance between disaster victims and the assigned shelter sites and a minimum utilization for open shelter sites. These constraints provide solutions that are preferable by both the victims and the DM (e.g. government authorities), respectively.

To be in accordance with the dataset provided by Kılıcı et al. (2015), we assume that the set of candidate shelter site locations is known in advance, all shelter sites have predetermined capacities and have previously assigned weights that denote their level of performance. Kılıcı et al. (2015) defines eligible shelter site locations, identifies the attributes of these shelter sites using ten different criteria, scales the values of respective criteria to com-

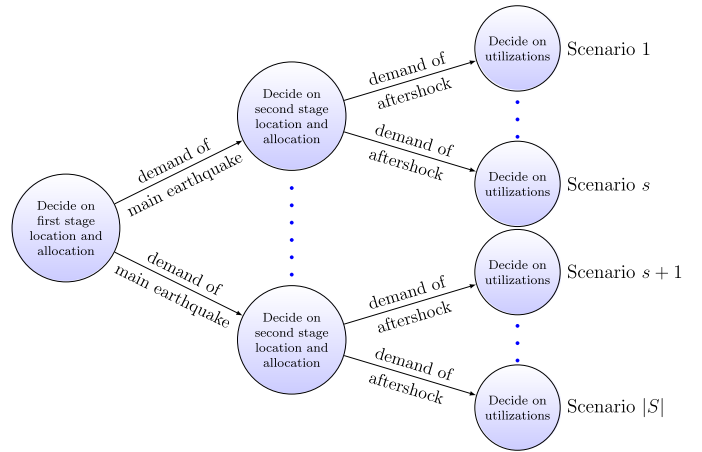


Fig. 2. Visualization of scenario structure.

mon units and finally calculates the weights of shelter sites as a convex combination of the scaled values.

We also assume that the population of each district is concentrated in its centroid. A significant assumption is on the capacity of the shelter sites - we assume that under no circumstances the capacity of a shelter site changes, i.e. the risk of losing convenience of any shelter site is non-existent.

In the formulation, we consider a finite set S of scenarios. Here, a scenario is a main earthquake-aftershock demand realization pair. Each scenario $s \in S$ occurs with a probability of p_s . This is visualized in Fig. 2. Each leaf, when traced back to root node, represents a scenario, i.e. main earthquake-aftershock scenario pair.

We use the following notation for the sets:

I : set of districts

J : set of candidate shelter sites

S : set of scenarios

S_s^2 : set of scenarios sharing the same history as scenario $s \in S$ up to second stage,

and for parameters:

w_j : weight of candidate shelter site $j \in J$; $w_j \in (0, 1]$

p_s : probability of scenario $s \in S$

τ_j : allowed tolerance for exceeding capacity of shelter site $j \in J$

- q_{is}^1 : number of people affected in district $i \in I$ under scenario $s \in S$ after the main earthquake
 q_{is}^2 : number of people affected in district $i \in I$ under scenario $s \in S$ after the aftershock
 d_{ij} : distance between district $i \in I$ and candidate shelter site $j \in J$
 α : risk-aversion parameter of CVaR
 c_j : capacity of shelter site $j \in J$.

For each district $i \in I$, the distances d_{ij} can be sorted non-decreasingly, thus providing an ordered sequence for the candidate shelter sites in terms of their distances to each district. We denote it by $j_i(r)$, the r -th closest candidate shelter site to district $i \in I$, $r \in \{1, \dots, |J|\}$.

Then we define the decision variables as:

$$\begin{aligned} x_j^1 &= \begin{cases} 1 & \text{if shelter site } j \text{ is established} \\ & \text{in first stage} \\ 0 & \text{otherwise} \end{cases} \quad \forall j \in J \\ y_{ij}^1 &= \begin{cases} 1 & \text{if district } i \text{ is assigned to} \\ & \text{shelter site } j \text{ in first stage} \\ 0 & \text{otherwise} \end{cases} \quad \forall i \in I, j \in J \\ x_{js}^2 &= \begin{cases} 1 & \text{if shelter site } j \text{ is established} \\ & \text{in second stage under scenario } s \\ 0 & \text{otherwise} \end{cases} \quad \forall j \in J, s \in S \\ y_{ijs}^2 &= \begin{cases} 1 & \text{if district } i \text{ is assigned to} \\ & \text{shelter site } j \text{ under scenario } s \\ & \text{in second stage} \\ 0 & \text{otherwise} \end{cases} \quad \forall i \in I, j \in J, s \in S \\ f_{js}^3 &= \text{overall utilization of shelter site} \\ & \quad j \text{ under scenario } s \quad \forall j \in J, s \in S. \end{aligned}$$

Recall the construction of this problem using the nearest assignment constraints. The definition of decision variables follows the same discussion. Since nearest assignment constraints are utilized, once the shelter sites are located, the assignment decisions are immediate. Therefore, the assignment decisions will be the same whether they are made before observing the demand or after observing the demand. But, to decide on the utilization of a shelter site, it is required to realize the uncertain demand for the whole process, which is in turn realized finally in the third stage. Hence follows the above definition of variables.

Additionally, for $j \in J$, we define random variables X_j^2 and F_j^3 . Let $x_{js}^2, s \in S$ be the realizations of the random variable X_j^2 where $X_j^2(s) = x_{js}^2$ for all $j \in J, s \in S$. And let $f_{js}^3, s \in S$ be the realizations of the random variable F_j^3 where $F_j^3(s) = f_{js}^3$ for all $j \in J, s \in S$. Then, we have the following three-stage stochastic MIP model:

$$P(S) = \min \sum_{s \in S} \sum_{j \in J} p_s \frac{1}{w_j} x_{js}^2 \quad (1)$$

s.t.

$$\sum_{j \in J} y_{ij}^1 = 1 \quad \forall i \in I \quad (2)$$

$$\sum_{k=r+1}^{|J|} y_{ij_i(k)}^1 + x_{j_i(r)}^1 \leq 1 \quad \forall i \in I, r \in \{1, \dots, |J| - 1\} \quad (3)$$

$$y_{ij}^1 \leq x_j^1 \quad \forall i \in I, j \in J \quad (4)$$

$$\sum_{j \in J} y_{ijs}^2 = 1 \quad \forall i \in I, s \in S \quad (5)$$

$$\sum_{k=r+1}^{|J|} y_{ij_i(k)s}^2 + x_{j_i(r)s}^2 \leq 1 \quad \forall i \in I, s \in S, r \in \{1, \dots, |J| - 1\} \quad (6)$$

$$y_{ijs}^2 \leq x_{js}^2 \quad \forall i \in I, j \in J, s \in S \quad (7)$$

$$x_j^1 \leq x_{js}^2 \quad \forall j \in J, s \in S \quad (8)$$

$$x_{js'}^2 = x_{js}^2 \quad \forall j \in J, s \in S, s' \in S_s^2 \quad (9)$$

$$\text{CVaR}_\alpha(F_j^3 - X_j^2) \leq \tau_j \quad \forall j \in J \quad (10)$$

$$f_{js}^3 = \frac{\sum_{i \in I} q_{is}^1 y_{ij}^1 + \sum_{i \in I} q_{is}^2 y_{ijs}^2}{c_j} \quad \forall j \in J, s \in S \quad (11)$$

$$x_j^1 \in \{0, 1\} \quad \forall j \in J \quad (12)$$

$$y_{ij}^1 \in \{0, 1\} \quad \forall i \in I, j \in J \quad (13)$$

$$x_{js}^2 \in \{0, 1\} \quad \forall j \in J, s \in S \quad (14)$$

$$y_{ijs}^2 \in \{0, 1\} \quad \forall i \in I, j \in J, s \in S. \quad (15)$$

The objective function (1) minimizes the expected weighted number of established shelter sites while aiming to establish shelter sites with higher weights. We achieve this goal using reciprocates of the shelter site weights. Constraints (2) make sure that every district is allocated to only one shelter site in the first stage. Constraints (3) are the nearest allocation constraints for the first stage as presented by Wagner and Falkson. Constraints (4) assure that, in the first stage, a district is assigned to a shelter site if this shelter site is established. For ease of representation, we denote constraints (2)–(4) as the “first stage allocation constraints”, so that constraints (5)–(7), which are only the projections of the same decisions, can be denoted as the “second stage allocation constraints”. Constraints (8) are to make sure that if shelter site $j \in J$ is established in the first stage, it should be kept open for any scenario at the second stage (i.e. a located shelter site cannot be closed). Constraints (9) are the non-anticipativity constraints. Constraints (10) are the CVaR constraints which check the utilizations of shelter sites and make sure that the configuration of established shelter sites meet the risk-aversion criterion. Constraints (11) define the overall utilization of a shelter site in the corresponding scenario. Lastly, constraints (12)–(15) are the domain constraints.

We introduce a more precise description of CVaR for continuous loss variables, as presented in Rockafellar and Uryasev (2000, 2002). Given that Z is a random cost:

$$\text{CVaR}_\alpha(Z) = \mathbb{E}[Z \mid Z \geq \text{VaR}_\alpha(Z)],$$

where

$$\text{VaR}_\alpha(Z) = \min_{\eta \in \mathbb{R}} \{\eta : \mathbb{P}\{Z \leq \eta\} \geq \alpha\},$$

and $\alpha \in (0, 1)$ is a preselected confidence level to tune the risk-aversion. So, $\text{CVaR}_\alpha(Z)$ is the conditional expected value of the losses exceeding the $\text{VaR}_\alpha(Z)$ at the confidence level α .

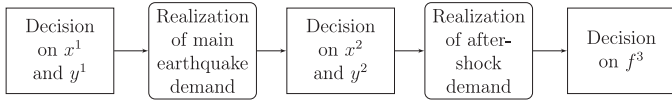


Fig. 3. Structure of the decision process.

A more general version of CVaR, which is defined for any random cost Z , discrete or continuous, is as follows (see Rockafellar and Uryasev, 2000):

$$\text{CVaR}_\alpha(Z) = \inf_{\eta \in \mathbb{R}} \left\{ \eta + \frac{1}{1-\alpha} \mathbb{E}([Z - \eta]_+) \right\} \quad (16)$$

where $[a]_+ = \max\{0, a\}$, $a \in \mathbb{R}$.

In this setting, we wish to control the risk of having over-utilized shelter sites. To do so, we introduce the discrete random variable $F_j^3 - X_j^2$ as the random cost (or loss). The realization of this difference under scenario s is positive (non-positive) when the realization of the utilization of shelter site j under scenario s is above (below) 100%. As the aim is to keep this loss, over-utilization when positive, as small as possible, we measure the risk of this loss using CVaR. We limit $\text{CVaR}_\alpha(F_j^3 - X_j^2)$ from above with τ_j , a parameter tuned by the DM as a secondary measure of risk-aversion – also a bound to control the upper tail of the loss distribution, and formally introduce the CVaR constraints (10).

To linearize the CVaR constraints (10), using the representation (16) and referring to Rockafellar and Uryasev (2000), we define two new types of continuous decision variables, z_{js} and η_j , $j \in J$, $s \in S$, and replace constraints (10) with constraints (17)–(20) in $P(S)$:

$$\eta_j + \frac{1}{1-\alpha} \sum_{s \in S} p_s z_{js} \leq \tau_j \quad \forall j \in J \quad (17)$$

$$z_{js} \geq f_{js}^3 - x_{js}^2 - \eta_j \quad \forall j \in J, s \in S \quad (18)$$

$$z_{js} \geq 0 \quad \forall j \in J, s \in S \quad (19)$$

$$\eta_j \text{ is free} \quad \forall j \in J. \quad (20)$$

In multi-stage stochastic models, for the scenarios having the same history up to a given stage, the decisions made at that stage must be the same. This is called non-anticipativity (see Birge and Louveaux, 2011 for details). In the proposed model, this means that scenarios having the same history up to second stage should share the same decisions at stage two. In other words, the assignment of districts to shelter sites and establishment of new shelter sites in the second stage cannot differ for scenarios sharing the same main earthquake demand realization. To force this on the proposed model, we utilize non-anticipativity constraints. Note that this type of constraints is not necessary for our first stage decisions as they do not depend on scenarios. Also note that we do not consider non-anticipativity constraints for the second stage allocation decisions, namely y_{ijs}^2 variables, since they are imposed by the nearest assignment constraints and non-anticipativity constraints on second stage shelter site establishment decisions.

To discuss the structure of non-anticipativity constraints in this context, in Fig. 3, we first visualize the decision process. Recall that a main earthquake triggers x^1 decisions and an aftershock triggers x^2 decisions (the indices are dropped for ease of notation). Also observe that assignment decisions are implicitly made with respect to location decisions and the utilization of shelter sites are finalized in the third stage. Since second stage shelter site location decisions are made after observing the main earthquake demand realization but before observing the realization of aftershock demand, these decisions should be the same for the scenarios sharing the same main earthquake demand realization. To force this,

we define set S_s^2 , which is the set of scenarios sharing the same history as scenario $s \in S$ up to second stage and use constraints (9).

In Fig. 3, location and allocation decisions in the first stage are followed by location and allocation decisions in the second stage, after the demand regarding the main shock is realized. Finally, after the demand regarding the aftershock is realized, the third stage decisions, shelter site utilizations, are finalized.

As discussed earlier in this section, we also add constraints to limit the maximum distance between the districts and assigned shelter sites and the minimum utilizations of open shelter sites to improve the solution qualities further. Constraints (21) and (22) limit the maximum distance between the districts and assigned shelter sites, stating that no district can be forced to travel a distance more than ρ :

$$y_{ij}^1 d_{ij} \leq \rho \quad \forall i \in I, j \in J \quad (21)$$

$$y_{ijs}^2 d_{ij} \leq \rho \quad \forall i \in I, j \in J, s \in S. \quad (22)$$

Constraints (23) and (24) limit the minimum utilizations of open shelter sites, stating that if at least one district is assigned to a shelter site, then that shelter site should be utilized at a level of at least v :

$$f_{js}^3 \geq v y_{ij}^1 \quad \forall i \in I, j \in J, s \in S \quad (23)$$

$$f_{js}^3 \geq v y_{ijs}^2 \quad \forall i \in I, j \in J, s \in S. \quad (24)$$

Then $P(S)$ is:

$$\begin{aligned} & \min (1) \\ & \text{s.t. (2) - (9), (11) - (15), (17) - (24).} \end{aligned}$$

4. Dataset

We model the demand uncertainty in this setting using a dataset consisting of scenarios for earthquake-aftershock pair. To the best of our knowledge, in the humanitarian logistics literature, even though there are many studies providing datasets on single (main –in the context of this study–) disasters (see e.g. Balcik and Beamon, 2008; Gunnec and Salman, 2007; Kilci et al., 2015; Li et al., 2011; Noyan et al., 2015; Verma and Gaukler, 2015) there is not any study that provides a dataset for both main and secondary disasters. Therefore, we devise a methodology for creating scenarios for a district of Istanbul, Turkey.

Throughout this study, we use the network of Kartal provided by Kilci et al. (2015) (see Figs. 4 and 5). Kartal has 25 candidate shelter site locations with corresponding capacities provided in Table 3. We create the dataset in accordance with the JICA study (JICA, 2002), where we assume that each main earthquake will be followed by 10 different aftershocks and all of the main earthquakes share the same epicenter, varying in magnitude. We propose 50 distinct main earthquakes and therefore a total of 500 disaster scenarios. We differentiate the earthquakes in this setting according to three features: epicenter, effect radius and percent affected ratio (*PAR*). The proposed methodology regards these features and, as discussed above, uses the same epicenter for every main earthquakes. For main earthquakes, we only decide on the effect radius and the proportion of the population in a district it affects, namely *PAR*. We assume that with a probability of 20%, the main earthquake will affect the districts in 3 km radius, and with a probability of 40% (40%), the main earthquake will affect the districts in 4 (5) km radius.

The corresponding *PAR* values along with their probabilities for the main earthquakes can be found in Table 4a, where $\mathcal{U}[a, b]$ denotes a continuous uniform distribution on the interval $[a, b]$ for which $a < b$. It is important to note that the districts are affected inversely proportional to their distances to the epicenter in the

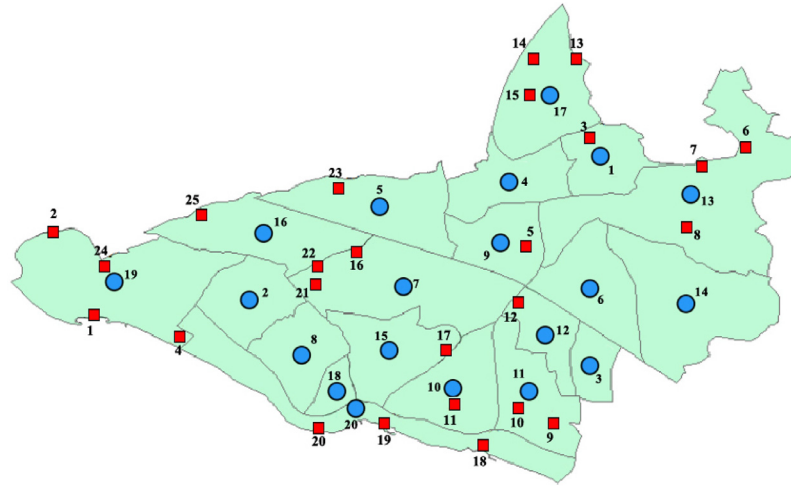


Fig. 4. Blue circles represent the demand points (districts) and red squares represent the candidate shelter site locations in Kartal. (For interpretation of the references to colour in this figure legend, the reader is referred to the web version of this article.)



Fig. 5. Location of Kartal in Istanbul.

cases of both main earthquakes and aftershocks. The same idea applies to the generation of aftershocks. But since aftershocks, as in the real setting, may depend on the main earthquake, we use the features of the main earthquake. We assume that the epicenter of the aftershock is within a circle, which is centered at the epicenter of the main earthquake and has a radius equal to the half of the effect radius of the main earthquake. The aftershock's effect radius is greater than the main earthquake's effect radius by a factor generated from $\mathcal{U}[0.3, 0.4]$, i.e. we multiply the effect radius of the main earthquake by $\mathcal{U}[1.3, 1.4]$ and obtain the interval for the effect radius of the aftershock. Note that also the *PAR* value of an aftershock is 20% lower than the main earthquake's *PAR* value. For example, if a main earthquake has an effect radius of 3 km, as in the first row of Table 4a, the aftershock's epicenter is within 1.5 km radius of the main earthquake's epicenter (see Fig. 6 for a visualization). The aftershock's effect radius is $3 \times \mathcal{U}[1.3, 1.4] = \mathcal{U}[3.9, 4.2]$, occurrence probabilities and *PAR* values are as in the first row of Table 4b. Note that this selection of parameters, for

Table 4a

Effect radius, occurrence probability and *PAR* values of main earthquakes.

Effect radius (km)	Occurrence probability	<i>PAR</i>
3	16%	$\mathcal{U}[0.4, 0.5]$
	50%	$\mathcal{U}[0.5, 0.6]$
	34%	$\mathcal{U}[0.6, 0.7]$
4	16%	$\mathcal{U}[0.5, 0.6]$
	50%	$\mathcal{U}[0.6, 0.7]$
	34%	$\mathcal{U}[0.7, 0.8]$
5	16%	$\mathcal{U}[0.6, 0.7]$
	50%	$\mathcal{U}[0.7, 0.8]$
	34%	$\mathcal{U}[0.8, 0.9]$

Table 4b

Effect radius, occurrence probability and *PAR* values of aftershocks.

Effect radius (km)	Occurrence probability	<i>PAR</i>
$\mathcal{U}[3.9, 4.2]$	16%	$\mathcal{U}[0.32, 0.40]$
	50%	$\mathcal{U}[0.40, 0.48]$
	34%	$\mathcal{U}[0.48, 0.56]$
$\mathcal{U}[5.2, 5.6]$	16%	$\mathcal{U}[0.40, 0.48]$
	50%	$\mathcal{U}[0.48, 0.56]$
	34%	$\mathcal{U}[0.56, 0.64]$
$\mathcal{U}[6.5, 7.0]$	16%	$\mathcal{U}[0.48, 0.56]$
	50%	$\mathcal{U}[0.56, 0.64]$
	34%	$\mathcal{U}[0.64, 0.72]$

magnitudes and effect radii, is data specific. We do not propose any empirical or theoretical relationship between characteristics of the aftershocks and the main shocks.

5. Multi-stage stochastic MIP results

In this section, we present the computational experiments conducted with the proposed mathematical model using the dataset

Table 3

Capacities of shelter sites.

Shelter site #	1	2	3	4	5	6	7	8	9
Capacity	24,000	45,000	25,000	60,000	60,000	25,000	30,000	75,000	25,600
Shelter site #	10	11	12	13	14	15	16	17	18
Capacity	100,000	30,000	62,500	60,000	50,000	30,625	30,000	75,000	45,000
Shelter site #	19	20	21	22	23	24	25		
Capacity		60,000	30,000	25,000	25,000	150,000	30,000	60,000	

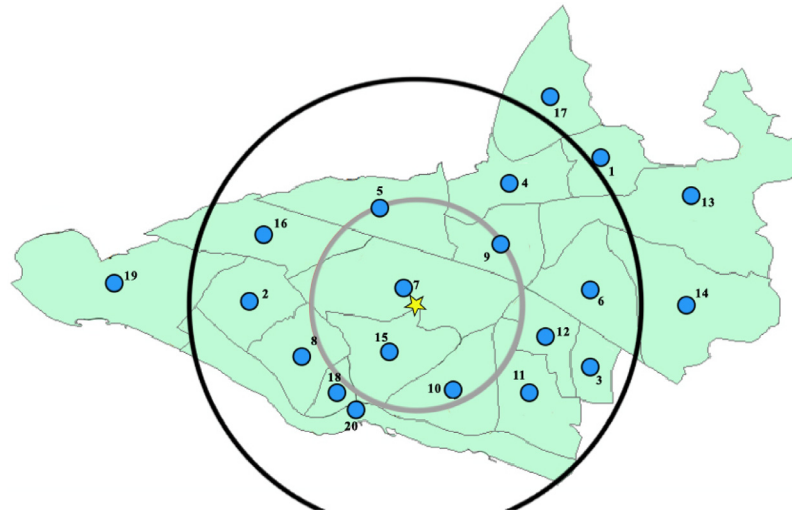


Fig. 6. Visualization of scenario generation methodology.

Table 5
Parameter settings for corresponding instance IDs.

(α, ν)	$\bar{\tau}$	ID
(0.90, 0.10)	0.05, ..., 0.25	1, ..., 5
(0.90, 0.15)	0.05, ..., 0.25	6, ..., 10
(0.95, 0.10)	0.05, ..., 0.25	11, ..., 15
(0.95, 0.15)	0.05, ..., 0.25	16, ..., 20

described in Section 4. The proposed model is coded in JAVA and solved using IBM CPLEX 12.7.1. All tests are run on a Linux OS with Dual Intel Xeon E5-2690 v4 14 Core 2.6GHz processor with 128 GB of RAM.

As discussed in previous sections, some of the parameters are left to be tuned by the DM. Two of these are risk-aversion level, namely α , and allowed tolerance for excess of capacity for each shelter site, namely $\tau_j, j \in J$. Note that $\forall j \in J$, we take τ_j the same and we will use $\bar{\tau}$ to denote values of all τ_j in this section.

Minimum utilization of established shelter sites, namely ν , provides the DM with the control of the overall utilizations of established shelter sites. The upper limit on the distance between disaster victims and the shelter sites is $\rho = 4$ (km) for all instances throughout this study. The parameter settings along with respective instance IDs are presented in Table 5. Note that $\bar{\tau}$ values differ by 5%, e.g. Instance ID 3 has $\bar{\tau} = 15\%$ and $(\alpha, \nu) = (0.90, 0.10)$.

For each test instance, we put a 6-hour time limit on CPLEX. The results are presented in Table 6. Note that the number of main earthquake-aftershock scenarios considered is 500.

In Table 6, the first column refers to the instance ID. The second column is the solution time of the corresponding instance in hours. If the corresponding instance cannot be solved to optimality in 6 hours, CPU time is denoted as "> 6". The third column denotes the optimality gap of the corresponding instance if it is not solved to optimality in 6 hours. Third and fourth columns refer to the configuration of the established shelter sites in first and second stages, respectively. Note that in the fourth column, the shelter sites established in the second stage are presented in their entirety, i.e. not all of them are established in every scenario but a subset of them are. The fifth column is the best objective value and is the optimal value of the corresponding test instance if it is solved to optimality. The last column is the average walk of the disaster victims to their allocated shelter site.

As seen in Table 6, most of the test instances are not solved to optimality in 6 hours. Two of the test instances, Instances 9

and 19, cannot be solved due to memory errors, denoted by "*" in the table. Those which are solved to optimality and used in comparative analyses are summarized in Tables 7a–7f. We present details on the locations of established shelter sites in each stage and their utilizations. Observe that we do not consider all of the test instances which are solved to optimality in this comparative analysis since we discuss the effect of different parameter settings and not all of the test instances are required for this.

In Tables 7a–7f, the leftmost column is the open shelter site's number. The second column states if the corresponding shelter site is established in the first or the second stage – the same note as previous table applies here, a subset of these second stage shelter sites is established in each scenario. The third, fourth and fifth columns denote the minimum, maximum and average utilizations of corresponding shelter site, respectively. Note that the minimum (maximum) utilization of a shelter site is its minimum (maximum) utilization over all scenarios. Lastly, the sixth column denotes the number of scenarios where the utilization of the corresponding shelter site has exceeded 100%.

To see the effect of minimum utilization, namely ν , on the solutions, we compare Instances 2 and 7, provided in Tables 7a and 7b, respectively. In Instance 2; $\nu = 10\%$ and in Instance 7; $\nu = 15\%$. Remaining two parameters, namely α and $\bar{\tau}$, are the same in both instances. As the minimum utilization increases, for this particular case, configuration of first stage shelter sites differs only by one shelter site, a bigger shelter site is opened instead of a smaller one, and its effect can be observed as a decrease in the average utilizations of unchanged set of open shelter sites. In the second stage, the model chooses to establish another shelter site under some scenarios.

The change in the set of open shelter sites in the first stage can be explained by the higher minimum utilization constraint. Utilizations of shelter sites 14 and 15 in Instance 2 are both smaller than 15%. Opening shelter site 13 instead of shelter site 14 in the first stage changes the nearest allocation configuration and provides even more districts to be allocated to shelter site 15 in the second stage so that its minimum utilization is more than 15%.

If we compare Instances 2 and 7 in terms of optimal value and average walk (see Table 6), we can say that Instance 2 provides a better quality solution than Instance 7 as its optimal value and average walk are smaller than those of Instance 7, in addition to the fact that the average utilizations of first stage shelter sites are higher. But, the solution time of Instance 2 is almost five times of the solution time of Instance 7.

Table 6

Test instances for 500 scenarios .

ID	CPU (hours)	Gap (%)	First stage shelter sites	Second stage shelter sites	Objective value	Average walk (m)
1	> 6	15.37	4, 10, 12, 14, 25	5, 15, 17, 21, 22	5.962	2203
2	5.6	opt.	4, 10, 12, 14, 25	15	5.761	2213
3	> 6	23.88	10, 12, 14, 25	1, 2, 4, 5, 15, 16, 24	5.466	2290
4	> 6	0.27	10, 13, 19, 25	5, 16, 24	5.001	2368
5	> 6	25.02	8, 10, 13, 25	16	4.960	2265
6	4.8	opt.	4, 10, 12, 13, 25	5, 15, 17, 22	6.067	2279
7	1.1	opt.	4, 10, 12, 13, 25	5, 15	5.866	2288
8	> 6	18.03	4, 10, 12, 13, 25	5, 15	5.866	2288
9	> 6	*	–	–	–	–
10	> 6	0.37	10, 14, 19, 25	3, 5, 16	4.972	2230
11	> 6	10.50	4, 10, 12, 14, 25	5, 15, 17, 21	6.003	2202
12	1.4	opt.	4, 10, 12, 14, 25	15, 17	5.801	2212
13	5	opt.	4, 10, 12, 14, 25	15	5.761	2213
14	> 6	6.81	10, 13, 19, 25	5, 16, 24	5.060	2362
15	> 6	6.58	10, 13, 19, 25	16, 24	4.934	2371
16	2.3	opt.	4, 10, 12, 13, 25	5, 15, 17, 21	6.108	2277
17	0.5	opt.	4, 10, 12, 13, 25	5, 15, 20	5.912	2287
18	0.6	opt.	4, 10, 12, 13, 25	5, 15	5.866	2288
19	> 6	*	–	–	–	–
20	> 6	0.88	10, 14, 19, 25	3, 5, 16	5.095	2224

Table 7a

Instance ID 2, 500 scenarios.

Shelter site	Stage	Minimum util (%)	Maximum util (%)	Average util (%)	Above 100% util
4	First	39.27	116.87	81	115
10	First	40.89	96.64	70.73	0
12	First	67.19	112	93.72	142
14	First	10.42	100.44	70.56	1
25	First	32.64	64.85	53.90	0
15	Second	11.51	48.85	29.05	0

Table 7b

Instance ID 7, 500 scenarios.

Shelter site	Stage	Minimum util (%)	Maximum util (%)	Average util (%)	Above 100% util
4	First	39.27	116.87	81	115
10	First	40.89	96.64	70.50	0
12	First	66.78	112	93.03	142
13	First	19.89	83.70	61.45	0
25	First	32.64	64.85	53.65	0
5	Second	16.80	60.35	32.74	0
15	Second	15.25	91.80	49.85	0

Table 7c

Instance ID 17, 500 scenarios.

Shelter site	Stage	Minimum util (%)	Maximum util (%)	Average util (%)	Above 100% util
4	First	39.27	113.93	80.80	114
10	First	40.89	94.27	70.35	0
12	First	66.78	112	93.03	142
13	First	19.89	83.70	61.45	0
25	First	32.64	64.85	53.65	0
5	Second	16.80	60.35	32.74	0
15	Second	15.25	91.80	49.85	0
20	Second	16.63	26.74	22.28	0

Table 7d

Instance ID 16, 500 scenarios.

Shelter site	Stage	Minimum util (%)	Maximum util (%)	Average util (%)	Above 100% util
4	First	39.27	112.66	79.32	43
10	First	40.89	92.27	69.05	0
12	First	66.78	107.35	91.71	87
13	First	19.89	83.70	61.32	0
25	First	32.64	63.53	53.40	0
5	Second	15.40	60.35	31.03	0
15	Second	15.25	91.80	49.85	0
17	Second	17.19	24.76	20.96	0
21	Second	58.65	77.26	65.83	0

Table 7e
Instance ID 18, 500 scenarios.

Shelter site	Stage	Minimum util (%)	Maximum util (%)	Average util (%)	Above 100% util
4	First	39.27	116.87	81	115
10	First	40.89	96.64	70.50	0
12	First	66.78	112	93.03	142
13	First	19.89	83.70	54.57	0
25	First	32.64	64.85	53.65	0
5	Second	16.80	60.35	32.74	0
15	Second	15.25	91.80	49.85	0

Table 7f
Instance ID 13, 500 scenarios.

Shelter site	Stage	Minimum util (%)	Maximum util (%)	Average util (%)	Above 100% util
4	First	39.27	116.87	81	115
10	First	40.89	96.64	70.73	0
12	First	67.19	112	93.72	142
14	First	10.42	100.44	70.56	1
25	First	32.64	64.85	53.90	0
15	Second	11.51	48.85	29.05	0

To see the effect of risk-aversion parameter, namely α , on the solutions, we compare Instances 7 and 17, provided in Tables 7b and 7c, respectively. In Instance 7; $\alpha = 90\%$ and in Instance 17; $\alpha = 95\%$, and the remaining two parameters, namely ν and $\bar{\tau}$, are the same for both instances. As the DM becomes more risk-averse (as α increases), the number of established shelter sites in the second stage increases to lower the higher utilizations of the established shelter sites of Instance 7, since we define the risk in this setting as the capacities of shelter sites being significantly exceeded.

It can be observed that the statistics on the utilizations do not differ in Instance 17 with respect to Instance 7 for shelter sites 12, 13 and 25 in the first stage and shelter sites 5 and 15 in the second stage. This is due to the nearest allocation constraints. In addition to Instance 7, only shelter site 20 is established in Instance 17 in the second stage. For districts allocated to shelter sites 12, 13 and 25 in the first stage and to shelter sites 5 and 15 in the second stage, opening shelter site 20 does not alter the nearest allocation configuration and therefore has no effect on the utilization statistics of aforementioned shelter sites. But some of the districts allocated to shelter sites 4 and 10 in the second stage can be allocated to shelter site 20 and thus it changes utilization statistics of shelter sites 4 and 10.

To see the effect of allowed tolerance parameter, namely $\bar{\tau}$, on the solutions, we compare Instances 17 and 16, provided in Tables 7c and 7d, respectively. In Instance 17; $\bar{\tau} = 10\%$ and in Instance 16; $\bar{\tau} = 5\%$. Remaining two parameters, namely α and ν , are the same for both instances. As discussed previously, $\bar{\tau}$ is used as a secondary measure of risk-aversion in this setting. But in contrast to α , increasing $\bar{\tau}$ decreases risk-aversion. First indicator of this fact is the decrease in the number of established shelter sites and the optimal value of Instance 17. Also, as a result of higher risk-aversion, the utilizations exceed 100% in less scenarios in Instance 16 with respect to Instance 17. Note that the Fig. 1a–1e in Section 3 are the visualizations of Instance 17.

Lastly, as an interesting observation, we present Instances 7 and 18, provided in Tables 7b and 7e, respectively. In both of the instances $\nu = 15\%$. With respect to α , Instance 18 is more risk-averse than Instance 7 as its α is bigger, but with respect to $\bar{\tau}$, Instance 7 is more risk-averse than Instance 18 as its $\bar{\tau}$ is smaller. And both instances have the same solution. The same phenomenon can also be observed in Instances 2 and 13, presented in Tables 7a and 7f, respectively. Instances 2 and 13 also share the same $\nu = 10\%$ and the same solutions.

As we cannot solve all of the instances to optimality within the specified time bound using 500 scenarios, in order to experiment, we decrease the cardinality of the scenario set and solve the model with smaller scenario sets. Since we propose that 10 different aftershocks may follow a main earthquake, to create smaller scenario sets, we first choose a smaller set of main earthquakes from the original set of main earthquakes and include the corresponding aftershocks to generate the whole scenario set. For example, for a set of 250 scenarios, we choose 25 main earthquakes out of 50 main earthquakes randomly, and include the aftershocks corresponding to those main earthquakes. The same methodology applies to generating a scenario set of cardinality 100. Table 8 presents the results of the test instances for a scenario set of cardinality 250.

We observe that as the cardinality of the scenario set decreases, the solution times decrease drastically and all of the instances can be solved to optimality. The longest solution time in the test runs with a scenario set of cardinality 250 is around 2.5 hours and the smallest solution time is 10 minutes.

In Tables 8 and 9, for most of the instances, it can be observed that the first stage shelter sites do not vary much but the second stage shelter sites do. In Table 8, Instances 3 and 13; 5 and 10; 8, 18 and 19; and 15 and 20 share the same solutions, respectively. In Table 9, Instances 2 and 12; 3 and 8; 5 and 15; 6 and 16; 9 and 19; and 10 and 20 share the same solutions, respectively. So as we decrease the size of the scenario set, varying nature of the earthquakes and the aftershocks cannot be represented thoroughly, and therefore we prefer to use larger datasets.

6. Solution methodology

As discussed previously, the solution times exceed 6-hour limit for most of the presented test instances with 500 scenarios. For instances solved to optimality in 6 hours, the average solution time is 2.7 hours where the average gap for test instances that cannot be solved to optimality in 6 hours is 10.77%, excluding the two instances that cannot be solved due to memory errors.

Since we need as many different scenarios as possible to represent the varying nature of earthquakes and aftershocks, we wish to solve the proposed model with a larger dataset and as we observe in Tables 8 and 9, the solution times significantly improve as the cardinality of the scenario set decreases. We utilize this fact in the construction of the proposed heuristic. We define R to be a reduced set of the original scenario set S , such that $R \subset S$.

Table 8

Test instances for 250 scenarios .

ID	CPU (sec)	First stage shelter sites	Second stage shelter sites	Objective value	Average walk (m)
1	4212	4, 10, 12, 13, 25	5, 17, 21	6.090	2285
2	1364	4, 10, 12, 13, 25	5, 17	5.786	2299
3	1086	4, 10, 12, 13, 25	5	5.745	2300
4	4035	10, 13, 19, 25	2, 5, 16, 24	5.194	2371
5	9263	10, 13, 19, 25	16	5.015	2380
6	1863	4, 10, 12, 13, 25	5, 15, 17, 20, 22	6.192	2284
7	684	4, 10, 12, 13, 25	5, 15, 20	5.888	2297
8	960	4, 10, 12, 13, 25	5, 15	5.842	2298
9	9247	4, 10, 13, 23	3, 5, 11, 15, 16, 17	5.503	2277
10	676	10, 13, 19, 25	16	5.015	2380
11	3186	4, 10, 12, 13, 25	5, 17, 21	6.149	2281
12	1112	4, 10, 12, 13, 25	5, 17	5.827	2298
13	880	4, 10, 12, 13, 25	5	5.745	2300
14	3229	10, 12, 13, 25	2, 4, 5, 16, 24	5.279	2383
15	1613	10, 13, 19, 25	5, 16	5.057	2377
16	1429	4, 10, 12, 13, 25	5, 15, 17, 21, 22	6.246	2280
17	602	4, 10, 12, 13, 25	5, 15, 20, 22	5.946	2294
18	739	4, 10, 12, 13, 25	5, 15	5.842	2298
19	2495	4, 10, 12, 13, 25	5, 15	5.842	2298
20	2286	10, 13, 19, 25	5, 16	5.057	2377

Table 9

Test instances for 100 scenarios.

ID	CPU (sec)	First stage shelter sites	Second stage shelter sites	Objective value	Average walk (m)
1	161	4, 10, 12, 13, 25	5, 22	6.165	2236
2	139	4, 10, 12, 13, 25	5, 17	6.016	2247
3	145	4, 10, 13, 19, 25	21	5.848	2276
4	118	10, 13, 19, 25	5, 16, 24	4.961	2337
5	84	10, 13, 19, 25	16, 24	4.855	2346
6	63	4, 10, 12, 13, 25	5, 15, 21	6.195	2247
7	64	4, 10, 12, 13, 25	15, 20	6.060	2258
8	81	4, 10, 13, 19, 25	21	5.848	2276
9	122	4, 10, 13, 19, 25	17	5.805	2279
10	55	10, 13, 19, 25	5, 16	4.855	2339
11	209	4, 10, 12, 13, 25	5, 21	6.165	2236
12	148	4, 10, 12, 13, 25	5, 17	6.016	2247
13	106	4, 10, 12, 13, 25	5	5.914	2250
14	113	8, 10, 13, 25	4, 5, 16	5.130	2284
15	86	10, 13, 19, 25	16, 24	4.855	2346
16	47	4, 10, 12, 13, 25	5, 15, 21	6.195	2247
17	64	4, 10, 12, 13, 25	15, 21	6.090	2253
18	68	4, 10, 12, 13, 25	15	5.945	2261
19	79	4, 10, 13, 19, 25	17	5.805	2279
20	53	10, 13, 19, 25	5, 16	4.855	2339

The proposed heuristic blends different approaches used in stochastic optimization. In each iteration of the proposed heuristic, we randomly create R , then solve $P(R)$ and obtain a first stage solution, namely x^{1*} . Then we fix the first stage variables in $P(S)$, namely x^1 , to x^{1*} and check for feasibility. Note that $P(R)$ is defined as a *group subproblem* with adjusted probabilities as Sandıkçı et al. (2013) propose. In $P(S)$, the probability of each scenario is equal to $1/|S|$, in $P(R)$, the probability of each scenario is equal to $1/|R|$.

Checking feasibility of x^{1*} , we should not obtain it in the next iterations. For this purpose, Ahmed (2013) suggests using no-good cuts to eliminate a solution from a solution pool. This is another approach we utilize in this heuristic. We perform this elimination by adding no-good cut constraint (25) to $P(R)$ in each iteration:

$$\sum_{j: x_j^{1*}=0} x_j^1 + \sum_{j: x_j^{1*}=1} (1 - x_j^1) \geq 1. \quad (25)$$

We store all no-good cuts in a cut pool C . After we conclude that x^{1*} is not feasible for $P(S)$, we add its no-good cut to the cut pool C . So in each iteration, we solve $P(R)$ with cut pool C , therefore, obtain a new set of open first stage shelter sites. The heuristic

stops when we find a set of open first stage shelter sites that is feasible for the original problem, i.e. x^{1*} is feasible for $P(S)$.

A more formal representation of the proposed heuristic is provided in Algorithm 1. Note that, hereafter, $\text{opt}[\cdot]$ implies the optimization of problem \cdot and gives the optimal value of it.

Algorithm 1. Heuristic methodology.

 Require: S .

```

1: Cut pool  $C \leftarrow \emptyset$ . Let  $\kappa$  be the cardinality of the reduced set.  $\text{bool} \leftarrow \text{TRUE}$ .
2: while  $\text{bool}$  do
3:   Create  $R \subset S$  randomly, with  $|R| = \kappa$ .
4:   Solve  $P(R)$  regarding  $C$ . Let  $x^{1*}$  be an optimal first stage decision of  $P(R)$ .
5:   Solve  $P(S)$  by fixing  $x^1 = x^{1*}$ .
6:   if  $P(S)$  is feasible then
7:      $\mathcal{V} := \text{opt}[P(S)]$ .  $\text{bool} \leftarrow \text{FALSE}$ .
8:   end if
9:   if  $\text{bool}$  then
10:    Add no-good cut  $\sum_{j: x_j^{1*}=0} x_j^1 + \sum_{j: x_j^{1*}=1} (1 - x_j^1) \geq 1$  to  $C$ .
11:   end if
12: end while
13: return  $\mathcal{V}$ 

```

The results of our heuristic are presented in Tables 10a – 10j. We report the solution time, optimality gap and iteration numbers

Table 10a
Configuration Set #1.

ID	Solution time (sec)	Gap (%)	# of iterations
2	539	0.1	3
6	653	0	3
7	581	0	3
12	658	0.1	3
13	621	0.1	3
16	621	0	3
17	582	0	3
18	441	0	3
Avg	587	0.038	3

Table 10b
Configuration Set #2.

ID	Solution time (sec)	Gap (%)	# of iterations
2	1657	9	1
6	841	0	4
7	686	0	4
12	802	0.1	4
13	1929	7	1
16	610	0	4
17	538	0	4
18	551	0	4
Avg	952	2.01	3.25

Table 10c
Configuration Set #3.

ID	Solution time (sec)	Gap (%)	# of iterations
2	413	0.1	2
6	421	0	2
7	276	0	2
12	487	0.1	2
13	445	0.1	2
16	271	0	2
17	260	0	2
18	292	0	2
Avg	358	0.038	2

Table 10d
Configuration Set #4.

ID	Solution time (sec)	Gap (%)	# of iterations
2	220	0.1	1
6	482	0	2
7	357	0	3
12	210	0.1	1
13	185	0.1	1
16	295	0	2
17	396	0	3
18	411	0	3
Avg	320	0.038	2

Table 10e
Configuration Set #5.

ID	Solution time (sec)	Gap (%)	# of iterations
2	207	0.1	1
6	337	0	1
7	545	0	4
12	204	0.1	1
13	2151	5	7
16	196	0	1
17	182	0	1
18	587	0	4
Avg	552	0.65	2.5

Table 10f
Configuration Set #6.

ID	Solution time (sec)	Gap (%)	# of iterations
2	195	0.1	1
6	191	0.1	1
7	167	0	1
12	201	0.3	1
13	210	0.1	1
16	173	0	1
17	170	0.1	1
18	139	0	1
Avg	181	0.088	1

Table 10g
Configuration Set #7.

ID	Solution time (sec)	Gap (%)	# of iterations
2	687	0.09	3
6	152	0	1
7	491	0	3
12	354	0.26	2
13	920	0.09	4
16	155	0	1
17	185	0.05	1
18	912	0	4
Avg	482	0.061	2.38

Table 10h
Configuration Set #8.

ID	Solution time (sec)	Gap (%)	# of iterations
2	818	0.09	4
6	338	0	2
7	476	0	3
12	1303	0.26	4
13	468	6.72	2
16	310	0	2
17	555	0.05	3
18	550	0	4
Avg	602	0.89	3

Table 10i
Configuration Set #9.

ID	Solution time (sec)	Gap (%)	# of iterations
2	161	0.09	1
6	144	0	1
7	137	0	1
12	167	0.26	1
13	1454	5.76	3
16	142	0	1
17	133	0.05	1
18	121	0	1
Avg	307	0.68	1.25

Table 10j
Configuration Set #10.

ID	Solution time (sec)	Gap (%)	# of iterations
2	1306	4.18	2
6	378	0	2
7	754	0	5
12	1436	0.26	5
13	403	5.26	2
16	311	0	2
17	740	0.05	5
18	956	0	7
Avg	786	1.22	3.75

for the instances that are solved to optimality in Table 6. As we choose set R randomly in each iteration, to discuss the effect of randomness and perform analyses on the selection of R , we perform the tests under 10 different configuration sets. Each configuration set includes a stream of random R sets. Note that in the

last rows of Tables 10a – 10j, we report the average value of each column.

In Tables 10a – 10j, the first column provides the instance IDs. Their corresponding solution times, optimality gaps, and number of iterations are provided in the second, third and fourth columns,

Table 11
Summary of results for $\kappa = 100$ and 500 scenarios with the proposed heuristic.

ID	Solution time (sec)	Gap (%)	# of iterations	First stage shelter sites	Second stage shelter sites	Objective value	Average walk (m)
1	708	− 0.06	1	4, 10, 12, 13, 25	5, 7, 21	5.958	2281
2	413	0.09	2	4, 10, 12, 13, 25	5	5.766	2289
3	906	0.40	1	4, 10, 13, 23	5, 15, 17	5.488	2253
4	200	0	1	10, 13, 19, 25	4, 5, 16, 24	5.001	2366
5	411	− 1.32	2	10, 13, 19, 25	16, 24	4.895	2370
6	421	0	2	4, 10, 12, 13, 25	5, 15, 17, 21	6.067	2279
7	276	0	2	4, 10, 12, 13, 25	5, 15	5.866	2288
8	372	0	2	4, 10, 12, 13, 25	5, 15	5.866	2288
9	371	*	2	4, 10, 13, 23	3, 5, 11, 15, 17	5.287	2274
10	759	0	4	10, 14, 19, 25	3, 5, 16	4.972	2230
11	339	0.09	1	4, 10, 12, 13, 25	5, 17, 22	6.008	2278
12	487	0.10	2	4, 10, 12, 13, 25	5, 17	5.807	2288
13	445	0.09	2	4, 10, 12, 13, 25	5	5.766	2289
14	385	− 0.01	1	10, 13, 19, 25	5, 16, 24	5.060	2364
15	448	0	2	10, 13, 19, 25	16, 24	4.934	2371
16	271	0	2	4, 10, 12, 13, 25	5, 15, 17, 21	6.108	2277
17	260	0	2	4, 10, 12, 13, 25	5, 15, 20	5.912	2287
18	292	0	2	4, 10, 12, 13, 25	5, 15	5.866	2288
19	334	*	2	4, 10, 13, 23	3, 5, 11, 15, 17	5.382	2271
20	506	0.03	3	10, 12, 13, 25	5, 15, 16	5.097	2379

respectively. Iteration number in a test corresponds to the number of times the smaller problem is solved. Note that $\kappa = 100$ and $|S| = 500$.

In Tables 10a – 10j, it is observed that generally the optimality gaps and the solution times for the instances are positively correlated. This is the main reason we present the results of the proposed heuristic with different configuration sets. The combination of scenarios in set R affects the performance of the proposed heuristic. But again, performing the proposed heuristic for 10 different random configuration sets – for Instances 2, 12 and 13, i.e. the instances for which we cannot find the optimal solution with any of the configuration sets – still has lower solution times with respect to the results in Table 6. So the proposed heuristic can be performed numerous times and the best solution it provides can be chosen as a near-optimal solution. Nonetheless, it should be kept in mind that it is costly to perform the heuristic methodology numerous times for the fine tuning.

In terms of performance among the 10 different configuration sets, it can be observed that configuration sets 1, 3 and 4 have the smallest average optimality gaps. We choose third configuration set to solve the remaining instances, namely the instances that cannot be solved to optimality in 6 hours. Note that the average computational time of third configuration set is between the other two sets, namely first and fourth configuration sets.

Table 11 provides the solution times, gaps – with respect to the solutions provided in Table 6, i.e. the best objective value – and the number of iterations along with the information on the solutions as in Table 6. A negative gap value states that the proposed heuristic provides a better objective value than the best objective value in Table 6, whereas a positive gap value states that the proposed heuristic provides a worse solution. Note that * denotes that the corresponding gap value cannot be calculated as CPLEX cannot find a feasible solution for those instances due to memory errors.

The objective values in Table 11 are similar to those in Table 6 and the proposed heuristic performs better in terms of solution times. The proposed heuristic also provides solutions for the instances where CPLEX cannot solve due to memory errors. Although we do not know the optimal solutions for some of the instances presented in Table 11, comparing with the results of CPLEX provided in 6 hours, we can say that the proposed heuristic performs well in terms of solution times as the maximum solution time is 15 minutes, averaging around 7 minutes. The reader should note that we disregard the time it takes to choose the configura-

tion set that will be used to solve the model, since it is up to the DM to choose the number of configuration sets to perform the initial comparison, and the cost of preprocessing changes accordingly.

7. Value of the three-stage model

To reiterate the value of using the proposed model in cases of consecutive disasters, we compare it with its *common* counterpart, where we separate the main earthquake and the aftershock in the decision making process, i.e. without relating the aftershocks to main earthquakes. We model this problem using two two-stage stochastic MILPs. The first program, namely F1, includes the decisions for the main earthquakes, and the second program, namely F2, includes the decisions for the aftershocks.

To solve this *common* counterpart problem, we first solve F1 considering only the main earthquake demand scenarios (realizations), i.e. we assume that the DM disregards the probability of having aftershocks while deciding for the locations of the shelter sites for the main earthquake. We then solve F2 for each set of possible aftershock demand realizations following each main earthquake demand realization.

Note that there are 50 different main earthquake demand realizations and 10 aftershock demand realizations following each main earthquake realization in the dataset. Therefore, we solve F1 once considering 50 different main earthquake demand realizations. We solve F2 50 times, each time with a different set of 10 aftershock demand realizations.

Here, we define new scenario sets, S_1 and \tilde{S}_s , $s \in S_1$. S_1 is the set of main earthquake demand scenarios (realizations) and $|S_1| = 50$ by construction of the proposed dataset. \tilde{S}_s is the set of aftershock demand scenarios (realizations) following the main earthquake scenario $s \in S_1$ and $|\tilde{S}_s| = 10$ for each $s \in S_1$ by construction. For each $j \in J$, we also define a discrete uniform random variable F_j^2 and let f_{js}^2 , $s \in S_1$ be the realizations of the random variable F_j^2 , where $F_j^2(s) = f_{js}^2$, $s \in S_1$. Also, for each $s \in S_1$ and $j \in J$, we define a discrete uniform random variable F_{js}^3 and let f_{jss}^3 , $\tilde{s} \in \tilde{S}_s$ be the realizations of it, where $F_{js}^3(\tilde{s}) = f_{jss}^3$, $\tilde{s} \in \tilde{S}_s$.

As the CVaR constraints (10) consider the losses resulting at the third stage, we cannot directly use the same τ_j values for the decomposed *common* counterpart problems. Therefore, we decompose the τ_j values as τ_j' for F1 and as τ_{js}'' , $s \in S_1$ for F2 in a given test using the optimal solutions in Table 6.

Referring to the original model and the definitions in Section 3:

$$\begin{aligned}
 F1(S_1) = \min \quad & \sum_{j \in J} \frac{1}{w_j} x_j^1 \\
 \text{s.t.} \quad & \\
 & (2) - (4), (12), (13), (21) \\
 & \text{CVaR}_\alpha(F_j^2 - x_j^1) \leq \tau_j' \quad \forall j \in J \\
 & f_{js}^2 = \frac{\sum_{i \in I} q_{is} y_{ij}^1}{c_j} \quad \forall j \in J, s \in S_1 \\
 & f_{js}^2 \geq v y_{ij}^1 \quad \forall i \in I, j \in J, s \in S_1,
 \end{aligned}$$

and $F2(\bar{S}_s)$ is:

$$\begin{aligned}
 F2(\bar{S}_s) = \min \quad & \sum_{j \in J} \frac{1}{w_j} x_{js}^2 \\
 \text{s.t.} \quad & \\
 & \sum_{j \in J} y_{ijs}^2 = 1 \quad \forall i \in I \\
 & \sum_{k=r+1}^{|J|} y_{ji(k)s}^2 + x_{ji(r)s}^2 \leq 1 \quad \forall i \in I, r \in \{1, \dots, |J|-1\} \\
 & y_{ijs}^2 \leq x_{js}^2 \quad \forall i \in I, j \in J \\
 & x_j^{1*} \leq x_{js}^2 \quad \forall j \in J \\
 & \text{CVaR}_\alpha(F_{js}^3 - x_{js}^2) \leq \tau_{js}'' \quad \forall j \in J \\
 & f_{js\bar{s}}^3 = \frac{\sum_{i \in I} q_{is} y_{ij}^{1*} + \sum_{i \in I} q_{i\bar{s}} y_{ij}^2}{c_j} \quad \forall j \in J, \bar{s} \in \bar{S}_s \\
 & y_{ijs}^2 d_{ij} \leq \rho \quad \forall i \in I, j \in J \\
 & f_{js\bar{s}}^3 \geq v y_{ijs}^2 \quad \forall i \in I, j \in J, \bar{s} \in \bar{S}_s \\
 & x_{js}^2 \in \{0, 1\} \quad \forall j \in J \\
 & y_{ijs}^2 \in \{0, 1\} \quad \forall i \in I, j \in J.
 \end{aligned}$$

Note that, both F1 and F2 are two-stage stochastic programming problems. In both formulations, location and allocation decisions are first stage decisions whereas utilization decisions are second stage decisions.

Note that we feed the solution provided from F1 to F2, so we denote x_j^1 and y_{ij}^1 as x_j^{1*} and y_{ij}^{1*} in F2, respectively, to indicate that

they are optimal decisions of F1. Also note that, we first solve F1 considering all the main earthquake demand realizations, i.e. for S_1 . Then, we solve $F2(\bar{S}_s)$ for the set of aftershock demand realizations corresponding to the main earthquake scenario $s \in S_1$. Obtained solutions are presented in Table 12.

The first column in Table 12 refers to the ID of the corresponding test instance. In the first row of the second column, we present the optimal value of the corresponding test instance, and in the second row of the second column we present the average of the optimal values of F2 problems, one F2 problem for each main earthquake demand realization. In the third and fourth columns, we present the maximum and average walk values of the proposed model and the *common* counterpart problem, respectively. In the last column, we denote the number of F2 problems that are infeasible, out of 50 problems.

As it can be observed in Table 12, there are some cases of infeasibilities caused by decomposing τ_j to τ_j' and τ_{js}'' , $s \in S_1$. In other words, in the proposed model, we consider all of the main earthquake-aftershock scenarios simultaneously and can meet the risk-aversion level for the whole planning horizon. But, we may fail to achieve the same level of risk-aversion using the *common* counterpart model even though more shelter sites are established overall.

In all of the instances, the proposed model dominates the *common* counterpart model in terms of the objective value but is sometimes dominated in terms of the average walks. This is mainly due to the large number of shelter sites established in the *common* counterpart model. Regardless, we can easily state that the proposed model performs better than the *common* counterpart model as the excess amount of established shelter sites does not seem to improve the average walk values considerably.

We present details of the comparison using Instance 16 as an example in Table 13. In the first column in Table 13, we average the number of shelter sites established over all scenarios. In the second column, we present the maximum utilization observed among all shelter sites over all scenarios. In the third column, we average the average shelter utilizations. And lastly, in the fourth column we present the number of scenarios where the utilization of a shelter site is above 100%.

As it is apparent from Table 13, it is more costly for the DM not to incorporate the aftershocks in the decision making process. In terms of the objective function and the number of established shelter sites, the proposed model outperforms the *common* counterpart model. The proposed model has a higher average utilization with smaller maximum utilization and smaller number of scenarios where a shelter site is utilized more than 100%. All these

Table 12

Comparison of objective values and walks of the proposed model and its *common* counterpart.

ID	Optimal value Average objective	Maximum walk (m)	Average walk (m)	# of infeasibilities
2	5.761	3571	2213	0
	8.679	3903	2251	
6	6.067	3903	2279	3
	8.699	3903	2228	
7	5.866	3903	2288	0
	8.741	3903	2245	
12	5.801	3571	2212	0
	8.778	3903	2250	
13	5.761	3571	2213	0
	7.919	3903	2272	
16	6.108	3903	2277	5
	8.348	3903	2228	
17	5.912	3903	2287	1
	8.396	3903	2251	
18	5.866	3903	2288	1
	7.746	3903	2273	

Table 13Comparison of the proposed model with the *common* counterpart model for Instance 16.

	Average # of overall shelter sites	Maximum util (%)	Average util (%)	# of scenarios above 100% util
Proposed model	5.34	112.66	58.05	130
<i>Common</i> counterpart model	7.93	120.63	54.67	146

statistics emphasize that the proposed model performs better than the *common* counterpart model.

8. Conclusion

In this study, we introduce a new modeling methodology to disaster operations management literature. We incorporate secondary disasters, e.g. aftershocks, to the shelter site location decisions after an earthquake has occurred and the demand is uncertain for both of the disasters. We devise a three-stage stochastic MIP model to mimic the real setting of an earthquake. In the first stage, before observing the actual demand of the main earthquake, we locate shelter sites. After the earthquake demand is realized in the second stage, the disaster victims travel to the nearest open shelter site. Note that we do not assign victims to the shelter sites, they choose the closest open shelter site and travel there without demand division. After the victims are located in the shelter sites, an aftershock might hit the area and create more disaster victims that require sheltering. Again, before observing the actual demand of the aftershock, we locate shelter sites in the second stage. Then, in the third stage, after the aftershock demand is realized, the aftershock victims travel to the nearest open shelter site.

We create a set of earthquake and aftershock scenarios for Kartal, Istanbul. We use the network of Kartal introduced in Kılıcı et al. (2015). We assume that 10 different aftershocks will follow each main earthquake and create a scenario set of cardinality 500, with 50 different main earthquake demand realizations.

As the solution times of the model with CPLEX are high, we propose a heuristic methodology. We improve the solution times drastically with the heuristic method while having small deviations from the optimal values of the instances for which we know the optimal solutions.

Comparing the proposed model with a *common* counterpart model, where we decompose the main earthquake and the aftershock and conduct the decision making without relating the aftershocks to main earthquakes, we show that it is important to consider secondary disasters while locating shelter sites for disaster operations management.

For future research, we believe that one can explore the risk of losing a shelter site, i.e. having its capacity decreased or having it destroyed, and can search for solutions that minimize the risk of such occurrences. Having the risk redefined, the mathematical model can be implemented for different problems in different disaster contexts, man-made or natural.

References

- Ahmed, S., 2013. A scenario decomposition algorithm for 0–1 stochastic programs. *Oper. Res. Lett.* 41 (6), 565–569.
- Alçada-Almeida, L., Tralhão, L., Santos, L., Coutinho-Rodrigues, J., 2009. A multiobjective approach to locate emergency shelters and identify evacuation routes in urban areas. *Geogr. Anal.* 41 (1), 9–29.
- Al Jazeera Turk, 2013. Earthquakes with mass casualties in Turkey (in Turkish). <http://www.aljazeera.com.tr/dosya/turkiyede-buyuk-depremler>
- Altay, N., Green, W.G., 2006. OR/MS Research in disaster operations management. *Eur. J. Oper. Res.* 175, 475–493.
- Balcık, B., Beamon, B.M., 2008. Facility location in humanitarian relief. *Int. J. Logist.* 11 (2), 101–121.
- Båth, M., 1965. Lateral inhomogeneities of the upper mantle. *Tectonophysics* 2, 483–514.
- Bayram, V., Tansel, B.Ç., Yaman, H., 2015. Compromising system and user interests in shelter location and evacuation planning. *Transp. Res. Part B* 72, 146–163.
- Bayram, V., Yaman, H., 2018. A stochastic programming approach for shelter location and evacuation planning. *RAIRO-Oper. Res.* 52 (3), 779–805.
- Birge, J.R., Louveaux, F., 2011. *Introduction to Stochastic Programming*. Springer Ser. Oper. Res. Financ. Eng. Springer, New York.
- Caunhye, A.M., Nie, X., Pokharel, S., 2012. Optimization models in emergency logistics: a literature review. *Socioecon. Plann. Sci.* 46, 4–13.
- Cavdur, F., Kose-Kucuk, M., Sebatli, A., 2016. Allocation of temporary disaster response facilities under demand uncertainty: an earthquake case study. *Int. J. Disaster Risk Reduct.* 19, 159–166.
- Chanta, S., Sangsawang, O., 2012. Shelter-site selection during flood disaster. *Lect. Note Manag. Sci.* 4, 282–288.
- Coutinho-Rodrigues, J., Tralhão, L., Alçada-Almeida, L., 2012. Solving a location-routing problem with a multiobjective approach: the design of urban evacuation plans. *J. Transp. Geogr.* 22, 206–218.
- Current, J., Daskin, M., Schilling, D., 2002. Discrete network location models. *Facility Locat.* 1, 81–118.
- EM-DAT, 2008. The international disaster database. Available at: <http://www.emdat.be/Database/Trends/trends.html>
- Galindo, G., Batta, R., 2013. Review of recent developments in OR/MS research in disaster operations management. *Eur. J. Oper. Res.* 230, 201–211.
- Grass, E., Fischer, K., 2016. Two-stage stochastic programming in disaster management: a literature survey. *Sur. Oper. Res. Manag. Sci.* 21 (2), 85–100.
- Gunnec, D., Salman, F., 2007. A two-stage multi-criteria stochastic programming model for location of emergency response and distribution centers. In: *International Network Optimization Conference*.
- Gutenberg, B., Richter, C.F., 1954. *Seismicity of the Earth and Related Phenomena*, 9. Princeton University Press, Princeton, p. 310.
- Görmez, N., Köksalan, M., Salman, F.S., 2011. Locating disaster response facilities in Istanbul. *J. Oper. Res. Soc.* 62, 1239–1252.
- Hoyos, M.C., Morales, R.S., Akhavan-Tabatabaei, R., 2015. OR Models with stochastic components in disaster operations management: a literature survey. *Comput. Ind. Eng.* 82, 183–197.
- JICA, 2002. The study on a disaster prevention/mitigation basic plan in Istanbul including seismic micronization in the Republic of Turkey final report. Japan Int. Cooperat. Agency.
- Kappes, M., Keiler, M., Glade, T., 2010. From single-to multi-hazard risk analysis: a concept addressing emerging challenges. In: *Proceedings of International Conference on Mountain Risks: Bringing Science to Society*. CERIG Editions, pp. 351–356.
- Kappes, M.S., Keiler, M., von Elverfeldt, K., Glade, T., 2012. Challenges of analyzing multi-hazard risk: a review. *Nat. Hazards* 64, 1925–1958.
- Kılıcı, F., Kara, B.Y., Bozkaya, B., 2015. Locating temporary shelter areas after an earthquake: a case for Turkey. *Eur. J. Oper. Res.* 243, 323–332.
- Kongsomsaksakul, S., Chao, Y., Anthony, C., 2005. Shelter location-allocation model for flood evacuation planning. *J. Eastern Asia Soc. Transp. Stud.* 6, 4237–4252.
- Kovács, G., Spens, K.M., 2007. Humanitarian logistics in disaster relief operations. *Int. J. Phys. Distribut. Logist. Manag.* 37 (2), 99–114.
- Leiras, A., de Brito Jr, I., Queiroz Peres, E., Rejane Bertazzo, T., Tsugunobu Yoshida Yoshizaki, H., 2014. Literature review of humanitarian logistics research: trends and challenges. *J. Humanitarian Logist. Supply Chain Manag.* 4 (1), 95–130.
- Li, A.C., Nozick, L., Xu, N., Davidson, R., 2012. Shelter location and transportation planning under hurricane conditions. *Transp. Res. Part E* 48 (4), 715–729.
- Li, L., Jin, M., Zhang, L., 2011. Sheltering network planning and management with a case in the gulf coast region. *Int. J. Prod. Econ.* 131 (2), 431–440.
- Liberatore, F., Pizarro, C., de Blas, C.S., Ortuño, M.T., Vitoriano, B., 2013. Uncertainty in humanitarian logistics for disaster management: a review. In: *Decision Aid Models for Disaster Management and Emergencies*. Springer, pp. 45–74.
- McLoughlin, D., 1985. A framework for integrated emergency management. *Public Admin. Rev.* 45, 165–172.
- Milliyet, 2011. Kızılay, Tarihinin En Büyük Afet Sevkiyatını Van'a Gerçekleştirdi (in Turkish). <http://www.milliyet.com.tr/kizilay--tarihinin-en-buyuk-afet-sevkiyatini-van-a-gerceklestirdi-gundem-1455140>
- Noyan, N., 2012. Risk-averse two-stage stochastic programming with an application to disaster management. *Comput. Oper. Res.* 39 (3), 541–559.
- Noyan, N., Balcık, B., Atakan, S., 2015. A stochastic optimization model for designing last mile relief networks. *Transp. Sci.* 50 (3), 1092–1113.
- Omori, F., 1894. On the aftershocks of earthquakes. *J. College Sci., Imp. Univ. Tokyo* 7, 111–200.
- Örgülü, G., Aktar, M., 2001. Regional moment tensor inversion for strong aftershocks of the august 17, 1999 Izmit earthquake (mw= 7.4). *Geophys. Res. Lett.* 28 (2), 371–374.
- Ortuño, M.T., Cristóbal, P., Ferrer, J.M., Martín-Campo, F.J., Muñoz, S., Tirado, G., Vitoriano, B., 2013. Decision aid models and systems for humanitarian logistics: a survey. In: *Decision Aid Models for Disaster Management and Emergencies*. Springer, pp. 17–44.

- Owen, S.H., Daskin, M.S., 1998. Strategic facility location: a review. *Eur. J. Oper. Res.* 111, 423–447.
- Özdamar, L., Ekinci, E., Küçükyazıcı, B., 2004. Emergency logistics planning in natural disasters. *Ann. Oper. Res.* 129 (1–4), 217–245.
- Rawls, C.G., Turnquist, M.A., 2010. Pre-positioning of emergency supplies for disaster response. *Transp. Res. Part B* 44 (4), 521–534.
- Rawls, C.G., Turnquist, M.A., 2011. Pre-positioning planning for emergency response with service quality constraints. *OR Spectrum* 33 (3), 481–498.
- Rockafellar, R.T., Uryasev, S., 2000. Optimization of conditional value-at-risk. *Journal of Risk* 2, 21–42.
- Rockafellar, R.T., Uryasev, S., 2002. Conditional value-at-risk for general loss distributions. *J. Bank. Finance* 26 (7), 1443–1471.
- Sandıkçı, B., Kong, N., Schaefer, A.J., 2013. A hierarchy of bounds for stochastic mixed-integer programs. *Math. Program.* 138 (1–2), 253–272.
- Simpson, N.C., Hancock, P.G., 2009. Fifty years of operational research and emergency response. *J. Oper. Res. Soc.* 60 (1), S126–S139.
- Snyder, L.V., 2006. Facility location under uncertainty: a review. *IIE Trans.* 38, 537–554.
- Su, Z., Zhang, G., Liu, Y., Yue, F., Jiang, J., 2016. Multiple emergency resource allocation for concurrent incidents in natural disasters. *Int. J. Disaster Risk Reduct.* 17, 199–212.
- Utsu, T., 1970. Aftershocks and earthquake statistics (1): some parameters which characterize an aftershock sequence and their interrelations. *J. Faculty Sci., Hokkaido Univer. Ser. 7, Geophys.* 3 (3), 129–195.
- Verma, A., Gaukler, G.M., 2015. Pre-positioning disaster response facilities at safe locations: an evaluation of deterministic and stochastic modeling approaches. *Comput. Oper. Res.* 62, 197–209.
- Wikipedia, 2018. List of aftershocks of april 2015 Nepal earthquake — wikipedia, the free encyclopedia. https://en.wikipedia.org/w/index.php?title=List_of_aftershocks_of_April_2015_Nepal_earthquake&oldid=860616190. Online; accessed 15-November-2018
- Wu, J., Cai, Y., Li, W., Feng, Q., 2017. Strong aftershock study based on coulomb stress triggering—a case study on the 2016 ecuador mw 7.8 earthquake. *Appl. Sci.* 7 (1), 88.
- Zhang, J.H., Li, J., Liu, Z.P., 2012. Multiple-resource and multiple-depot emergency response problem considering secondary disasters. *Expert Syst. Appl.* 39, 11066–11071.